



Publication Year	2020
Acceptance in OA	2025-03-17T13:11:45Z
Title	The baryon density of the Universe from an improved rate of deuterium burning
Authors	Mossa, V., Stöckel, K., Cavanna, F., Ferraro, F., Aliotta, M., Barile, F., Bemmerer, D., Best, A., Boeltzig, A., Brogini, C., Bruno, C. G., Caciolli, A., Chillery, T., Ciani, G. F., Corvisiero, P., Csedreki, L., Davinson, T., Depalo, R., Di Leva, A., Elekes, Z., Fiore, E. M., Formicola, A., Fülöp, Zs., Gervino, G., Guglielmetti, A., Gustavino, C., Gyürky, G., Imbriani, G., Junker, M., Kievsky, A., Kochanek, I., Lugaro, M., Marcucci, L. E., Mangano, G., Marigo, P., Masha, E., Menegazzo, R., Pantaleo, F. R., Patocchio, V., Perrino, R., Piatti, D., Pisanti, O., Prati, P., Schiavulli, L., STRANIERO, Oscar, Szücs, T., Takács, M. P., Trezzi, D., Viviani, M., Zavatarelli, S.
Publisher's version (DOI)	10.1038/s41586-020-2878-4
Handle	http://hdl.handle.net/20.500.12386/36851
Journal	NATURE
Volume	587

The baryon density of the Universe from an improved rate of deuterium burning

<https://doi.org/10.1038/s41586-020-2878-4>

Received: 7 May 2020

Accepted: 16 September 2020

Published online: 11 November 2020

 Check for updates

V. Mossa¹, K. Stöckel^{2,3}, F. Cavanna^{4,26}, F. Ferraro^{4,5}, M. Aliotta⁶, F. Barile¹, D. Bemmerer², A. Best^{7,8}, A. Boeltzig^{9,10}, C. Broggini¹¹, C. G. Bruno⁶, A. Cacioli^{11,12}, T. Chillery⁶, G. F. Ciani^{9,10}, P. Corvisiero^{4,5}, L. Csedreki^{9,10}, T. Davinson⁶, R. Depalo¹¹, A. Di Leva^{7,8}, Z. Elekes¹³, E. M. Fiore^{1,14}, A. Formicola¹⁰, Zs. Fülöp¹³, G. Gervino^{15,16}, A. Guglielmetti^{17,18}, C. Gustavino¹⁹, G. Gyürky¹³, G. Imbriani^{7,8}, M. Junker¹⁰, A. Kievsky²⁰, I. Kochanek¹⁰, M. Lugaro^{21,22}, L. E. Marcucci^{20,23}, G. Mangano^{7,8}, P. Marigo^{11,12}, E. Masha^{17,18}, R. Menegazzo¹¹, F. R. Pantaleo^{1,24}, V. Patricchio¹, R. Perrino^{1,27}, D. Piatti¹¹, O. Pisanti^{7,8}, P. Prati^{4,5}, L. Schiavulli^{1,14}, O. Straniero^{10,25}, T. Szücs², M. P. Takács^{2,3}, D. Trezzi^{17,18}, M. Viviani²⁰ & S. Zavatarelli⁴✉

Light elements were produced in the first few minutes of the Universe through a sequence of nuclear reactions known as Big Bang nucleosynthesis (BBN)^{1,2}. Among the light elements produced during BBN^{1,2}, deuterium is an excellent indicator of cosmological parameters because its abundance is highly sensitive to the primordial baryon density and also depends on the number of neutrino species permeating the early Universe. Although astronomical observations of primordial deuterium abundance have reached percent accuracy³, theoretical predictions^{4–6} based on BBN are hampered by large uncertainties on the cross-section of the deuterium burning $D(p,\gamma)^3\text{He}$ reaction. Here we show that our improved cross-sections of this reaction lead to BBN estimates of the baryon density at the 1.6 percent level, in excellent agreement with a recent analysis of the cosmic microwave background⁷. Improved cross-section data were obtained by exploiting the negligible cosmic-ray background deep underground at the Laboratory for Underground Nuclear Astrophysics (LUNA) of the Laboratori Nazionali del Gran Sasso (Italy)^{8,9}. We bombarded a high-purity deuterium gas target¹⁰ with an intense proton beam from the LUNA 400-kilovolt accelerator¹¹ and detected the γ -rays from the nuclear reaction under study with a high-purity germanium detector. Our experimental results settle the most uncertain nuclear physics input to BBN calculations and substantially improve the reliability of using primordial abundances to probe the physics of the early Universe.

The theoretical description of Big Bang nucleosynthesis (BBN) is based on the standard cosmological model (hereafter, the Λ cold dark matter (Λ CDM) model, where Λ is the cosmological constant²), which assumes a homogeneous and isotropic Universe governed by general relativity and by the standard model of particle physics. Under these assumptions, BBN predicts the abundances of primordial nuclides, mainly ^2H (hereafter, D), ^3He , ^4He and ^7Li , as a function of one parameter only—the density of ordinary matter, or the baryon density, $\Omega_b h^2$, where h is the reduced Hubble constant (see Fields et al.¹² for a recent review). Therefore, a comparison between the observed primordial abundances and those predicted by the BBN can be used to constrain this fundamental quantity. Yet an independent evaluation of $\Omega_b h^2$ can also be obtained

by measuring the anisotropies in the cosmic microwave background (CMB), which is the relic electromagnetic radiation left over from the Big Bang.

It should be noted that $\Omega_b h^2$ from the CMB reflects the baryon density of the Universe at the re-combination epoch, some 380,000 years after the Big Bang. According to the Λ CDM model, the baryon density can only vary as a result of the expansion of the Universe, so that its present-day value inferred from either the CMB or BBN should be the same. Therefore, the evaluation of $\Omega_b h^2$ based on BBN alone is critical as it can either support the Λ CDM model or point to new physics between the BBN and CMB epochs². Here we present a new evaluation of $\Omega_b h^2$ from BBN based on improved experimental nuclear physics inputs

¹INFN, Sezione di Bari, Bari, Italy. ²Helmholtz-Zentrum Dresden-Rossendorf, Dresden, Germany. ³Technische Universität Dresden, Dresden, Germany. ⁴INFN, Sezione di Genova, Genoa, Italy.

⁵Università degli Studi di Genova, Genoa, Italy. ⁶School of Physics and Astronomy, SUPA, University of Edinburgh, Edinburgh, UK. ⁷Università degli Studi di Napoli “Federico II”, Naples, Italy.

⁸INFN, Sezione di Napoli, Naples, Italy. ⁹Gran Sasso Science Institute, L’Aquila, Italy. ¹⁰INFN, Laboratori Nazionali del Gran Sasso (LNGS), Assergi, Italy. ¹¹INFN, Sezione di Padova, Padua, Italy.

¹²Università degli Studi di Padova, Padua, Italy. ¹³Institute for Nuclear Research (Atomki), Debrecen, Hungary. ¹⁴Dipartimento Interateneo di Fisica, Università degli Studi di Bari, Bari, Italy.

¹⁵Università degli Studi di Torino, Turin, Italy. ¹⁶INFN, Sezione di Torino, Turin, Italy. ¹⁷Università degli Studi di Milano, Milan, Italy. ¹⁸INFN, Sezione di Milano, Milan, Italy. ¹⁹INFN, Sezione di

Roma, Rome, Italy. ²⁰INFN, Sezione di Pisa, Pisa, Italy. ²¹Konkoly Observatory, Research Centre for Astronomy and Earth Sciences, MTA Centre for Excellence, Budapest, Hungary. ²²Institute

of Physics, ELTE Eötvös Loránd University, Budapest, Hungary. ²³Dipartimento di Fisica “E. Fermi”, Università degli Studi di Pisa, Pisa, Italy. ²⁴Dipartimento Interateneo di Fisica, Politecnico di

Bari, Bari, Italy. ²⁵INAF Osservatorio Astronomico d’Abruzzo, Teramo, Italy. ²⁶Present address: INFN, Sezione di Torino, Turin, Italy. ²⁷Present address: INFN, Sezione di Lecce, Lecce, Italy.

✉e-mail: carlo.gustavino@roma1.infn.it; sandra.zavatarelli@ge.infn.it

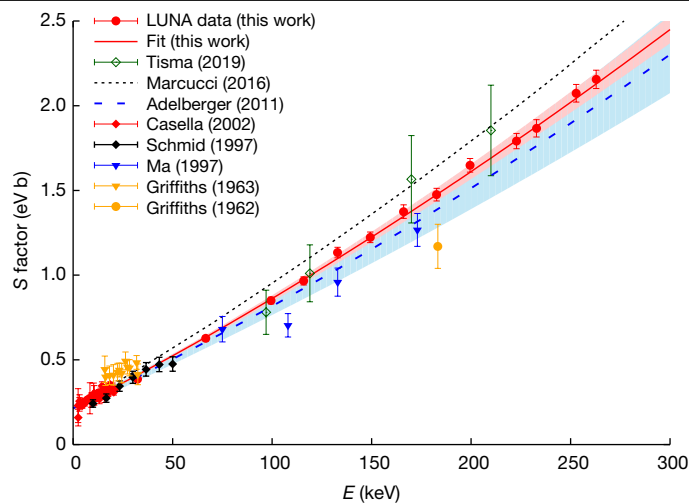


Fig. 1 | The S factor of the $D(p,\gamma)^3\text{He}$ reaction. At BBN energies ($E_{\text{cm}} \approx 30\text{--}300$ keV), the new LUNA results (filled red circles, with total (statistical + systematic) error bars) indicate a faster deuterium destruction compared with a best fit¹⁹ (blue dashed line) of previous experimental data, but a slower destruction compared with theoretical calculations¹⁸ (black dotted line). At BBN energies, the best fit (red solid line, equation (2)) obtained in this work is entirely dominated by the LUNA data. The fit includes all experimental data^{13–16,29–31} (note that those by Warren et al.³⁰ and Geller et al.³¹ lie outside the energy range shown here). Bands represent the 68% confidence level.

obtained at the Laboratory for Underground Nuclear Astrophysics (LUNA)^{8,9} of the National Institute for Nuclear Physics (INFN) Laboratori Nazionali del Gran Sasso (Italy).

Of the elements produced during the BBN, deuterium (D) is an excellent indicator of cosmological parameters in the early Universe because its abundance is the most sensitive to the baryon density $\Omega_b h^2$ and also depends on the radiation density, usually expressed in terms of the effective number N_{eff} of neutrino species². As deuterium is almost exclusively produced during BBN, and is destroyed only during stellar evolution, its primordial abundance can be obtained from astrophysical sites not affected by stellar evolution⁴. The best determination of the deuterium abundance is at present obtained by analysing the light spectra of quasars crossing pristine gas clouds at high redshift. Recent astronomical observations³ have reached excellent precision and provide a weighted mean value of the primordial deuterium abundance relative to hydrogen, $(D/H)_{\text{obs}} = (2.527 \pm 0.030) \times 10^{-5}$, with a 1% uncertainty³ (hereafter, quoted errors are at 68% confidence level unless stated otherwise). By contrast, theoretical predictions of D/H based on BBN, $(D/H)_{\text{BBN}}$, are less clear: Coc et al.⁵ reported a value in agreement with observations, but with a higher uncertainty, whereas Pitrou et al.⁴ reported a value in tension with observations, albeit with a similar precision. Improving such predictions requires an accurate knowledge of the nuclear reaction rates involved in the synthesis of deuterium: specifically, production via the well known $p(n,\gamma)\text{D}$ process, and destruction via the $D(d,n)^3\text{He}$, $D(d,p)^3\text{H}$ and $D(p,\gamma)^3\text{He}$ reactions. Of these, the $D(p,\gamma)^3\text{He}$ reaction^{3–6} carries the largest uncertainties because of insufficient experimental data at relevant BBN energies. Although the $D(p,\gamma)^3\text{He}$ cross-section, or equivalently its S factor (see Methods section ‘ $D(p,\gamma)^3\text{He}$ cross-section measurements at LUNA’), is well known¹³ at low energies, $E \approx 3\text{--}20$ keV (energies are in the centre-of-mass system unless stated otherwise), higher-energy data^{14–17} are affected by systematic uncertainties of 9% or more. In addition, a recent ab initio theoretical calculation¹⁸ disagrees at the level of 20–30% with a widely used S-factor best fit¹⁹ to selected datasets^{13–15,20} and at the level of about 8% with a fit by Iliadis et al.²¹. As a result, BBN predictions of primordial deuterium abundance remain unsatisfactory, which calls for improved measurements of the $D(p,\gamma)^3\text{He}$ reaction cross-section over a wide energy range^{3–6,12}.

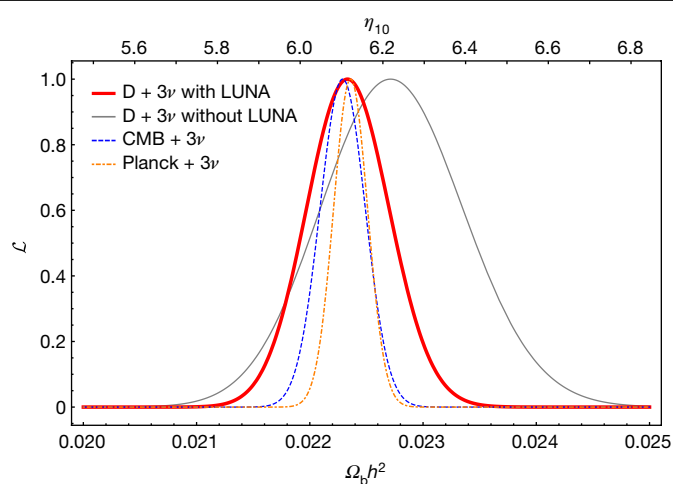


Fig. 2 | Likelihood distribution of the baryon density and baryon-to-photon ratio. The red curve ($D + 3\nu$ with LUNA) shows the distribution of the baryon density obtained using the new LUNA S factor for the predicted deuterium abundance $(D/H)_{\text{BBN}}$. Note the factor of two reduction in the uncertainty, compared with the distribution based on the previous S factor¹⁹ (grey curve, $D + 3\nu$ without LUNA). Our new determination of $\Omega_b h^2$ is now in much better agreement with the value obtained from CMB data alone¹² (blue dashed curve, $\text{CMB} + 3\nu$) and with the best determination of baryon density obtained by the Planck Collaboration⁷ from CMB data combined with additional observational inputs and with the theoretical dependence of primordial ^4He on baryon density (orange dot-dashed curve, $\text{Planck} + 3\nu$). η_{10} , baryon-to-photon ratio.

The new measurement of the $D(p,\gamma)^3\text{He}$ cross-section discussed in this paper was performed at the LUNA 400-kV accelerator¹¹, a world-leading facility to study nuclear reactions at the lowest-energies frontier of nuclear astrophysics. The million-fold reduction in cosmic-ray muons of the deep-underground location⁸ and a careful commissioning¹⁰ of the experimental setup aimed at minimizing all sources of systematic errors have led to $D(p,\gamma)^3\text{He}$ cross-section data of unprecedented precision and with overall uncertainties below 3% over the measured energy region ($E = 32\text{--}263$ keV), relevant to BBN energies ($E = 30\text{--}300$ keV; Methods). As shown in Fig. 1, the new data represent a substantial improvement compared with previous work^{14,15,17}. Our new S-factor best fit (red solid line) implies a destruction of deuterium that is faster compared with the best fit¹⁹ of previous experimental data (blue dashed curve) and slower compared with predictions based on the ab initio calculation¹⁸ (black dotted curve).

To explore the impact of our $D(p,\gamma)^3\text{He}$ S factor on the predicted primordial deuterium abundance, we used the second release²² of the numerical BBN code PARthENoPE. Under the assumption of the ΛCDM model, with^{23,24} $N_{\text{eff}} = 3.045$, we performed a Bayesian likelihood analysis (Methods) to derive $\Omega_b h^2$ using the observed deuterium abundance, $(D/H)_{\text{obs}}$, and the theoretical behaviour of $(D/H)_{\text{BBN}}$ (now including the new LUNA data). We obtain $\Omega_b h^2(\text{BBN}) = 0.02233 \pm 0.00036$. As shown in Fig. 2, this value is a factor of two more precise than that obtained using a previous S factor¹⁹ and now in much better agreement with the $\Omega_b h^2$ based on CMB data¹² (see values in Table 1). The use of BBN deuterium alone as a baryometer has now approached a precision comparable to that obtained from CMB analyses^{7,12}. The fact that the present-day values of $\Omega_b h^2(\text{BBN})$ and $\Omega_b h^2(\text{CMB})$ are fully consistent with each other (Table 1) offers evidence of the validity of the ΛCDM model adopted here.

We note that if we use the baryon density provided by the Planck Collaboration⁷, we derive a theoretical prediction on deuterium abundance $(D/H)_{\text{BBN}} = (2.52 \pm 0.03 \pm 0.06) \times 10^{-5}$, in excellent agreement with astronomical observations³ $(D/H)_{\text{obs}} = (2.527 \pm 0.030) \times 10^{-5}$. The quoted errors on $(D/H)_{\text{BBN}}$ stem from the propagation of uncertainties in the baryon density (first error) and the nuclear rates (second error).

Table 1 | Mean values and 68% confidence level ranges for $\Omega_b h^2$ (with relative uncertainties δ) and N_{eff}

	$\Omega_b h^2$	δ (%)	N_{eff}
D + 3v (without LUNA data)	0.02271 ± 0.00062	2.73	3.045
D + 3v (with new LUNA data)	0.02233 ± 0.00036	1.61	3.045
CMB + 3v	0.02230 ± 0.00021^a	0.94	3.045
Planck + 3v	0.02236 ± 0.00015	0.67	3.045
(D + CMB)	0.02224 ± 0.00022	0.99	2.95 ± 0.22
(D + Y_p)	0.0221 ± 0.0006	2.71	$2.86^{+0.28}_{-0.27}$

The first two lines show the results obtained from the likelihood analyses performed in this study, without and with the new $D(p, \gamma)^3\text{He}$ S factor obtained at LUNA and with N_{eff} fixed to its standard value^{23,24} of 3.045. The third and fourth lines show results obtained, respectively, using CMB data alone¹² (CMB + 3v) and CMB data combined with the theoretical dependence of primordial ^4He on baryon density⁷ (Planck + 3v). The last two lines correspond to cases in which both $\Omega_b h^2$ and N_{eff} are left as free parameters and the likelihood functions are constrained by either the deuterium abundance and a prior distribution on $\Omega_b h^2$, (D + CMB) case, or the observed and predicted abundances of both deuterium and helium, (D + Y_p) case (in both cases the predicted deuterium abundance takes into account our new LUNA results; see Methods for details).

^aQuoted in Fields et al.¹² as 0.022298 ± 0.000214 .

To probe the existence of physics beyond the ΛCDM model, we performed likelihood analyses in which both $\Omega_b h^2$ and N_{eff} were left as free parameters. As the deuterium abundance alone cannot be used to constrain $\Omega_b h^2$ and N_{eff} when they are both varied, we considered two cases with additional inputs. In the first case, hereafter (D + CMB), we used the deuterium abundance, both observed $(D/H)_{\text{obs}}$ and predicted $(D/H)_{\text{BBN}}$, combined with a Gaussian distribution of the CMB baryon density⁷, with mean value and uncertainty as obtained by the Planck Collaboration without constraining N_{eff} . In the second case, hereafter (D + Y_p), we used observed and predicted values of both the deuterium abundance and the ^4He mass fraction²⁵, Y_p , without constraining $\Omega_b h^2$. The results are shown in Fig. 3 as contour plots in the plane N_{eff} versus $\Omega_b h^2$. Numerical values at the 68% confidence level are reported in Table 1. We note that at the 99% confidence level, we obtain $N_{\text{eff}} = 2.95^{+0.61}_{-0.57}$ and $N_{\text{eff}} = 2.86^{+0.75}_{-0.67}$ for the (D + CMB) and (D + Y_p) cases, respectively. Our largest values of N_{eff} deviate by at most 20% from its standard value^{23,24} $N_{\text{eff}} = 3.045$. This implies a maximum amount of ‘dark radiation’, due to particle species that are not foreseen by the Standard model of particle physics, in agreement with the Planck Collaboration⁷.

Although the (D + CMB) and (D + Y_p) cases discussed above lead to consistent outcomes, the (D + Y_p) result depends on the value of Y_p used. In our analysis, we adopted the value of Aver et al.²⁵, which is close to those of Peimbert et al.²⁶, Valerdi et al.²⁷ and the recommended value in Tanabashi et al.². When the much higher Y_p value of Izotov et al.²⁸ is used, we obtain $N_{\text{eff}} = 3.60^{+0.45}_{-0.43}$ (99% confidence level).

To conclude, we have measured the $D(p, \gamma)^3\text{He}$ reaction cross-section to an unprecedented precision of better than 3% by exploiting the million-fold reduction in cosmic-ray muons at LUNA. The new S factor has led to a remarkable improvement in the evaluation of the present-day baryon density, $\Omega_b h^2$, using standard BBN alone. Our value is now in better agreement with the one derived from the analysis of the CMB anisotropies and provides further support to the standard cosmological model. When combined with additional inputs such as the CMB baryon density or the primordial helium abundance, our data also provide a strong experimental foundation to constrain the amount of dark radiation.

Online content

Any methods, additional references, Nature Research reporting summaries, source data, extended data, supplementary information, acknowledgements, peer review information; details of author contributions

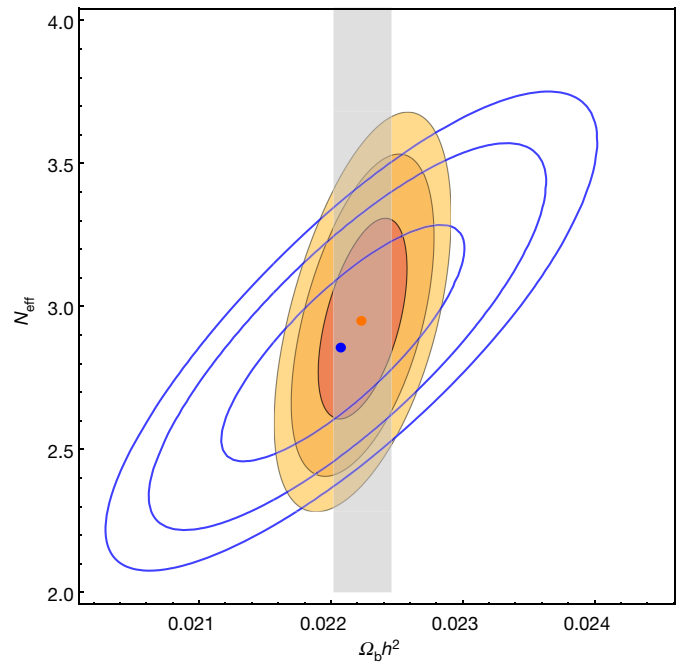


Fig. 3 | Likelihood contours (at 68%, 95% and 99% confidence levels) on the N_{eff} versus $\Omega_b h^2$ plane. Orange filled contours are obtained for the (D + CMB) case using the observed deuterium abundance³ $(D/H)_{\text{obs}}$ and the adopted Planck distribution on baryon density⁷ (grey vertical band at the 68% confidence level). Blue contours correspond to the (D + Y_p) case, as obtained from a likelihood analysis with observed abundances of deuterium³ and ^4He mass fraction²⁵, Y_p , and the corresponding BBN theoretical predictions (see Methods for details). Central values for each case are indicated by dots.

and competing interests; and statements of data and code availability are available at <https://doi.org/10.1038/s41586-020-2878-4>.

- Cyburtt, R. H., Fields, B. D., Olive, K. A. & Yeh, T.-H. Big Bang nucleosynthesis: present status. *Rev. Mod. Phys.* **88**, 015004 (2016).
- Tanabashi, M. et al. Review of particle physics. *Phys. Rev. D* **98**, 030001 (2018).
- Cooke, R., Pettini, M. & Steidel, C. One percent determination of the primordial deuterium abundance. *Astrophys. J.* **855**, 102 (2018).
- Pitrou, C., Coc, A., Uzan, J. & Vangioni, E. Precision Big Bang nucleosynthesis with improved helium-4 predictions. *Phys. Rep.* **754**, 1–66 (2018).
- Coc, A. et al. New reaction rates for improved primordial D/H calculation and the cosmic evolution of deuterium. *Phys. Rev. D* **92**, 123526 (2015).
- Di Valentino, E. et al. Probing nuclear rates with Planck and BICEP2. *Phys. Rev. D* **90**, 023543 (2014).
- Aghanim, N. et al. Planck 2018 results. VI. Cosmological parameters. *Astron. Astrophys.* **641**, A6 (2020).
- Broggini, C., Bemmerer, D., Caciolli, A. & Trezzi, D. LUNA: status and prospects. *Prog. Part. Nucl. Phys.* **98**, 55–84 (2018).
- Cavanna, F. & Prati, P. Direct measurement of nuclear cross-section of astrophysical interest: results and perspectives. *Int. J. Mod. Phys. A* **33**, 1843010–1843042 (2018).
- Mossa, V. et al. Setup commissioning for an improved measurement of the $D(p, \gamma)^3\text{He}$ cross section at Big Bang nucleosynthesis energies. *Eur. Phys. J. A* **56**, 144 (2020).
- Formicola, A. et al. The LUNA II 400kV accelerator. *Nucl. Instrum. Methods Phys. Res. A* **507**, 609–616 (2003).
- Fields, B. D., Olive, K. A., Yeh, T.-H. & Young, C. Big-Bang nucleosynthesis after Planck. *J. Cosmol. Astropart. Phys.* **03**, 010 (2020).
- Casella, C. et al. First measurement of the $d(p, \gamma)^3\text{He}$ cross section down to the solar Gamow peak. *Nucl. Phys. A* **706**, 203–216 (2002).
- Ma, L. et al. Measurements of $^1\text{H}(d, \gamma)^3\text{He}$ and $^2\text{H}(p, \gamma)^3\text{He}$ at very low energies. *Phys. Rev. C* **55**, 588–596 (1997).
- Griffiths, G., Larson, E. & Robertson, L. The capture of protons by deuterons. *Can. J. Phys.* **40**, 402–411 (1962).
- Schmid, G. et al. The $^2\text{H}(p, \gamma)^3\text{He}$ and $^1\text{H}(d, \gamma)^3\text{He}$ reactions below 80 keV. *Phys. Rev. C* **56**, 2565–2581 (1997).
- Tiřma, I. et al. Experimental cross section and angular distribution of the $^2\text{H}(p, \gamma)^3\text{He}$ reaction at Big-Bang nucleosynthesis energies. *Eur. Phys. J. A* **55**, 137 (2019).
- Marcucci, L., Mangano, G., Kievsky, A. & Viviani, M. Implication of the proton-deuteron radiative capture for Big Bang nucleosynthesis. *Phys. Rev. Lett.* **116**, 102501 (2016).
- Adelberger, E. et al. Solar fusion cross sections. II. The pp chain and CNO cycles. *Rev. Mod. Phys.* **83**, 195–245 (2011).

20. Schmid, G. et al. Effects of non-nucleonic degrees of freedom in the $D(\vec{p},\gamma)^3\text{He}$ and the $p(\vec{d},\gamma)^3\text{He}$ reactions *Phys. Rev. Lett.* **76**, 3088–3091 (1996).
21. Iliadis, C., Anderson, K. S., Coc, A., Timmes, F. X. & Starrfield, S. Bayesian estimation of thermonuclear reaction rates. *Astrophys. J.* **831**, 107 (2016).
22. Consiglio, R. et al. PArthENoPE reloaded. *Comput. Phys. Commun.* **233**, 237–242 (2018).
23. De Salas, P. & Pastor, S. Relic neutrino decoupling with flavour oscillations revisited. *J. Cosmol. Astropart. Phys.* **07**, 051 (2016).
24. Mangano, G. et al. Relic neutrino decoupling including flavour oscillations. *Nucl. Phys. B* **729**, 221–234 (2005).
25. Aver, E., Olive, K. A., & Skillman, E. D. The effects of He I $\lambda 10830$ on helium abundance determinations. *J. Cosmol. Astropart. Phys.* **07**, 011 (2015).
26. Peimbert, A., Peimbert, M. & Luridiana, V. The primordial helium abundance and the number of neutrino families. *Rev. Mex. Astron. Astrofis.* **52**, 419–424 (2016).
27. Valerdi, M., Peimbert, A., Peimbert, M. & Sixtos, A. Determination of the primordial helium abundance based on NGC 346, an H II region of the Small Magellanic Cloud. *Astrophys. J.* **876**, 98 (2019).
28. Izotov, Y. I., Thuan, T. X. & Guseva, N. G. The primordial deuterium abundance of the most metal-poor damped Ly α system. *Mon. Not. R. Astron. Soc.* **445**, 778–793 (2014).
29. Griffiths, G., Lal, M. & Scarfe, C. The reaction $D(p,\gamma)^3\text{He}$ below 50 keV. *Can. J. Phys.* **41**, 724–736 (1963).
30. Warren, J. B., Erdman, K. L., Robertson, L. P., Axen, D. A. & Macdonald, J. R. Photodisintegration of ^3He near the threshold. *Phys. Rev.* **132**, 1691–1692 (1963).
31. Geller, K., Muirhead, E. & Cohen, L. The $^2\text{H}(p,\gamma)^3\text{He}$ reaction at the breakup threshold. *Nucl. Phys. A* **96**, 397–400 (1967).

Publisher's note Springer Nature remains neutral with regard to jurisdictional claims in published maps and institutional affiliations.

© The Author(s), under exclusive licence to Springer Nature Limited 2020

D(p,γ)³He cross-section measurements at LUNA

The cross-section of the D(p,γ)³He reaction (Q -value = 5.493 MeV, where the Q -value is the energy released or absorbed by the nuclear reaction and can be obtained from the mass difference between reacting and resulting nuclei) was measured in direct kinematics using a high-intensity (100–300 μ A) proton beam from the LUNA 400-kV accelerator¹¹ over the full dynamic energy range $E_p = 50$ –395 keV, corresponding to centre-of-mass energies $E = 33$ –263 keV. The beam was sent onto a windowless and extended gas target containing high-purity (99.999%) deuterium maintained at a pressure of $P = 0.3$ mbar by a system of three differential pumping stages. A copper calorimeter³² at the end of the gas target stopped the beam and allowed its intensity to be measured. Gamma rays from the D(p,γ)³He reaction were detected by a large high-purity germanium detector mounted in close geometry under the target chamber and facing its centre. Full details of the experimental setup and its commissioning have been described elsewhere¹⁰.

For an extended gas target of length L , the cross-section of the D(p,γ)³He reaction can be expressed in terms of experimentally measurable quantities as:

$$\sigma(E) = \frac{N_\gamma(E)}{N_p \int_0^L \rho(z) \epsilon(z, E_\gamma) W(z) dz} \quad (1)$$

where $N_\gamma(E)$ is the net number of detected γ -rays at a given interaction energy E , N_p is the number of incident protons, $\rho(z)$ is the number density of target atoms as a function of interaction position z along the target, $\epsilon(z, E_\gamma)$ is the γ -ray detection efficiency and $W(z)$ is a term accounting for the angular distribution of the emitted γ -rays.

Under experimental conditions at LUNA, the γ -rays emitted by the D(p,γ)³He reaction have energies $E_\gamma = 5.5$ –5.8 MeV, that is, far away from the energy of the commonly used radioactive sources. Thus, a measurement of the detection (photopeak) efficiency was performed using different-energy γ -rays emitted in cascade from the well known resonant reaction ¹⁴N($p,\gamma_1\gamma_2$)¹⁵O. Efficiency corrections were validated by extensive Monte Carlo simulations as described in detail in Mossa et al.¹⁰.

To reduce the uncertainty on the final cross-section, we performed dedicated measurements to minimize the systematic errors associated with each term of equation (1).

A typical γ -ray spectrum taken at a proton beam energy $E_p = 50$ keV is shown in Extended Data Fig. 1. We note that the γ -ray background at LUNA is three to four orders of magnitude lower than on the Earth's surface⁸ in the region of interest ($E_\gamma \approx 5.5$ –5.8 MeV) for the D(p,γ)³He reaction. As a result, the counting statistical error could be kept below 1% at all beam energies. The main source of beam-induced background was due to the ¹⁹F($p,\alpha\gamma$)¹⁶O reaction from the interaction of protons with fluorine contaminant usually present on collimators along the gas target and on the calorimeter¹⁰ (beam dump). This beam-induced background ($E_\gamma < 7$ MeV) was found to be negligible at beam energies $E_p < 250$ keV. At higher energies, approaching the well known ¹⁹F($p,\alpha\gamma$)¹⁶O resonance at $E_p = 340$ keV, the beam-induced background was carefully accounted for in dedicated control runs in which (inert) ⁴He gas was used instead of deuterium. A sample spectrum taken at the highest beam energy studied ($E_p = 395$ keV) is shown in Extended Data Fig. 2.

The cross-section results obtained at LUNA for the D(p,γ)³He reaction are shown in Fig. 1 (and summarized in Extended Data Table 1) in the form of the astrophysical S factor. This is defined as³³ $S(E) = E\sigma(E)\exp(2\pi\eta)$, where E is the energy of interaction, $\sigma(E)$ is the energy dependent cross-section and η is the Sommerfeld parameter $\eta(E) = Z_1Z_2\alpha(\mu c^2/2E)^{1/2}$ (where Z_1 and Z_2 are the atomic numbers of the interacting nuclei, α is the fine structure constant, μ is the reduced mass and c is the speed of light). We achieved an overall systematic uncertainty lower than 3%, with the main contributions arising from uncertainties in the beam current (1%),

target density profile (1.1%) and efficiency (2%), as described in Mossa et al.¹⁰. We note that our new experimental data are close to a previous fit²¹ (not shown in Fig. 1) based on a Bayesian analysis of previous selected experimental datasets.

Our new S factor was used together with other datasets^{13–16,29–31} to arrive at the best fit:

$$S(E) = (0.2121 + 5.973 \times 10^{-3}E + 5.449 \times 10^{-6}E^2 - 1.656 \times 10^{-9}E^3) \text{ eV b} \quad (2)$$

(with centre-of-mass E in keV and $1 \text{ b} = 10^{-24} \text{ cm}^2$) shown in Fig. 1 (red solid line). The fit was performed over a broad centre-of-mass energy range $E = 2$ –2,000 keV, following the approach of Serpico et al.³⁴. At BBN energies, the fit is entirely dominated by the new LUNA data reported here, owing to their increased precision compared with previous studies. We obtain a reduced χ^2 of 1.049. The uncertainties on the fit (red band in Fig. 2) are given by:

$$(\Delta S(E))^2 = (1.4 \times 10^{-5} + 2.97 \times 10^{-8}E^2 + 4.80 \times 10^{-13}E^4 + 1.12 \times 10^{-19}E^6) \text{ eV}^2 \text{ b}^2 \quad (3)$$

(with E in keV). The correlation among data points of the same dataset was properly taken into account³⁴ by introducing a single normalization factor for each dataset, constrained by the so-called penalty factor in the χ^2 .

As the Universe expands, BBN takes place over a temperature range of the nucleon-photon plasma $k_B T \approx 100$ –20 keV, with k_B being the Boltzmann constant and T the temperature. To better assess the energy range where precise measurements of the D(p,γ)³He cross-section have the largest impact in improving the accuracy of theoretical predictions of primordial deuterium abundance relative to hydrogen, $(D/H)_{\text{BBN}}$, we used a sensitivity function (see, for example, Nollett et al.³⁵), defined as the ratio of the logarithmic derivatives of the D/H abundance and the corresponding S factor:

$$\zeta(E) = \frac{\delta \log (D/H)_{\text{BBN}}}{\delta \log S(E)} \quad (4)$$

Specifically, we varied the S factor in 10-keV energy bins, over a broad energy region of 10–500 keV, and calculated the corresponding thermal rate (obtained by convolution with the Maxwell–Boltzmann distribution) bin by bin as a function of energy. The corresponding yield of deuterium was obtained using the PARthENoPE code²² (see also ‘Bayesian likelihood analysis’ below). The results are shown in Extended Data Fig. 3. We note that the sensitivity curve remains above 25% of the maximum variation in a range $E = 20$ –240 keV, with the deuterium abundance being most sensitive to the D(p,γ)³He cross-section at $E \approx 80$ keV, that is, in a region where our precision underground measurements are essential. Our values of the D(p,γ)³He thermal rate and their uncertainties are provided in Extended Data Table 2.

Bayesian likelihood analysis

To study the effect of the new LUNA D(p,γ)³He S factor on primordial deuterium produced during BBN, we have computed the corresponding thermal rate and updated it (O. Pisanti et al., manuscript in preparation) in the second release of the BBN code PARthENoPE²². The rates of the D(d,n)³He and D(d,p)³H have also been updated following the publication of new datasets³⁶, although their inclusion has a negligible effect (O. Pisanti et al., manuscript in preparation) on the uncertainty on the $(D/H)_{\text{BBN}}$ value presented in this work. Starting from conditions of nuclear statistical equilibrium, PARthENoPE solves a set of coupled ordinary differential equations that follow the departure from chemical equilibrium of nuclear species and determines their asymptotic abundances as a function of several input cosmological parameters, such as the baryon density $\Omega_b h^2$, the effective number of neutrino species

N_{eff} , the value of the cosmological constant and neutrino chemical potentials (see, for example, Pisanti et al.³⁷ for details).

The reduced uncertainty of the LUNA results affects the precision of BBN deuterium prediction and can constrain the baryon density. In a first analysis, we assume a standard BBN scenario and fix the value of the relativistic degrees of freedom to photons and three active neutrino species ($N_\nu = 3$) corresponding to a contribution $N_{\text{eff}} = 3.045$ in the energy density of neutrinos, conventionally given⁶ as $\rho_\nu = \frac{7}{8} \left(\frac{4}{11}\right)^{4/3} \rho_\gamma N_{\text{eff}}$ (with ρ_γ being the photon density). We use $(D/H)_{\text{BBN}}$ as a function of $\Omega_b h^2$ and the deuterium abundance inferred from astronomical observations $(D/H)_{\text{obs}}$. The likelihood function is:

$$\mathcal{L}_{D+3\nu}(\Omega_b h^2) = \exp \left[-\frac{[(D/H)_{\text{BBN}}(\Omega_b h^2) - (D/H)_{\text{obs}}]^2}{2[\sigma_{\text{BBN}}^2(\Omega_b h^2) + \sigma_{\text{obs}}^2]} \right] \quad (5)$$

where σ_{BBN} is the propagated error on the deuterium yield due to the experimental uncertainties on nuclear reactions and σ_{obs} is the uncertainty on the astronomical observations.

We performed two other analyses in which both $\Omega_b h^2$ and N_{eff} were free to vary and constrained the likelihood function $\mathcal{L}_D(\Omega_b h^2, N_{\text{eff}})$ with other astrophysical inputs. In one case, (D + CMB), we used the deuterium abundance (both predicted and observed) and assumed a Gaussian distribution on the baryon density, $\mathcal{L}_{\text{CMB}}(\Omega_b h^2)$, corresponding to the latest Planck Collaboration value⁷, $\Omega_b h^2(\text{CMB}) = 0.02224 \pm 0.00022$, obtained without constraining N_{eff} . The likelihood function is now expressed as:

$$\mathcal{L}_{D+\text{CMB}}(\Omega_b h^2, N_{\text{eff}}) = \mathcal{L}_{\text{CMB}}(\Omega_b h^2) \exp \left[-\frac{[(D/H)_{\text{BBN}}(\Omega_b h^2, N_{\text{eff}}) - (D/H)_{\text{obs}}]^2}{2[\sigma_{\text{BBN}}^2(\Omega_b h^2, N_{\text{eff}}) + \sigma_{\text{obs}}^2]} \right] \quad (6)$$

In the other case, (D + Y_p), we used BBN predictions and observed abundances of both deuterium and ^4He mass fraction ($Y_p = 0.2449 \pm 0.0040$ from astronomical observations²⁵) together with the most recent² neutron lifetime ($\tau_n = 879.4 \pm 0.6$ s), which carries the largest uncertainty on the theoretical prediction of ^4He primordial abundance. No prior distribution was assumed on the baryon density. In this case, the likelihood function is the product of two exponential functions: one for deuterium as that appearing in equation (6), and a similar one for ^4He .

Data availability

Experimental data taken at LUNA are proprietary to the collaboration but can be made available from the corresponding authors upon

reasonable request. Values of the thermonuclear reaction rate for smaller temperature steps can be obtained upon request to O.P. (e-mail: pisanti@na.infn.it). Source data are provided with this paper.

Code availability

The PARthENoPE code used for BBN calculations can be made available upon request to O.P. (e-mail: pisanti@na.infn.it).

32. Ferraro, F. et al. A high-efficiency gas target setup for underground experiments, and redetermination of the branching ratio of the 189.5 keV $^{22}\text{Ne}(p,\gamma)^{23}\text{Na}$ resonance. *Eur. Phys. J. A* **54**, 44 (2018).
33. Rolfs, C. & Rodney, W. *Cauldrons in the Cosmos* (Univ. Chicago Press, 1988).
34. Serpico, P. D. et al. Nuclear reaction network for primordial nucleosynthesis: a detailed analysis of rates, uncertainties and light nuclei yields. *J. Cosmol. Astropart. Phys.* **2004**, 010 (2004).
35. Nollett, K. M. & Burles, S. Estimating reaction rates and uncertainties for primordial nucleosynthesis. *Phys. Rev. D* **61**, 123505 (2000).
36. Tumino, A. et al. New determination of the $^2\text{H}(d,p)^3\text{H}$ and $^2\text{H}(d,n)^3\text{He}$ reaction rates at astrophysical energies. *Astrophys. J.* **785**, 96 (2014).
37. Pisanti, O. et al. PARthENoPE: public algorithm evaluating the nucleosynthesis of primordial elements. *Comput. Phys. Commun.* **178**, 956–971 (2008).

Acknowledgements We thank D. Ciccotti for accelerator operation and maintenance, for mechanical setups and servicing of the vacuum systems during the course of the experiment; M. D'Incecco for work on custom electronics; M. De Deo for the data acquisition system; G. Sobrero for the new gas target control panel. We also thank the mechanical workshop at LNGS, INFN Bari and Dipartimento Interateneo di Fisica Bari. This work was supported by INFN, with contributions from DFG (BE4100/4-1), Helmholtz Association (ERC-RA-0016), NKFIH (K120666), COST Association (ChETEC CA16117), STFC-UK, University of Naples Compagnia di San Paolo grant STAR, research grant number 2017W4HA7S NAT-NET: 'Neutrino and Astroparticle Theory Network' under the programme PRIN 2017 funded by the Italian Ministry of Education, University and Research (MIUR) and INFN Iniziativa Specifica TAsP. R.D. acknowledges funding from the Italian Ministry of Education, University and Research (MIUR) through the 'Dipartimenti di eccellenza' project Science of the Universe.

Author contributions The experiment at LUNA was proposed by C.G. and coordinated by F.C. and D.T.; P.C., C.G., S.Z. and V.M. planned the setup; S.Z. and P.C. developed the Monte Carlo simulations; S.Z., F.C., P.C., C.G., V.M., K.S. and F.F. led the data analysis. Other authors contributed to the data-taking over a period of two years and to discussion and interpretation of the results obtained. M.J. also had overall responsibility for the accelerator operations and the underground site. G.M. and O.P. performed all BBN calculations and Bayesian analyses. L.E.M., A.K., M.V. performed ab initio calculations. M.A., F.C., C.G., G.M. and O.P. also wrote the paper.

Competing interests The authors declare no competing interests.

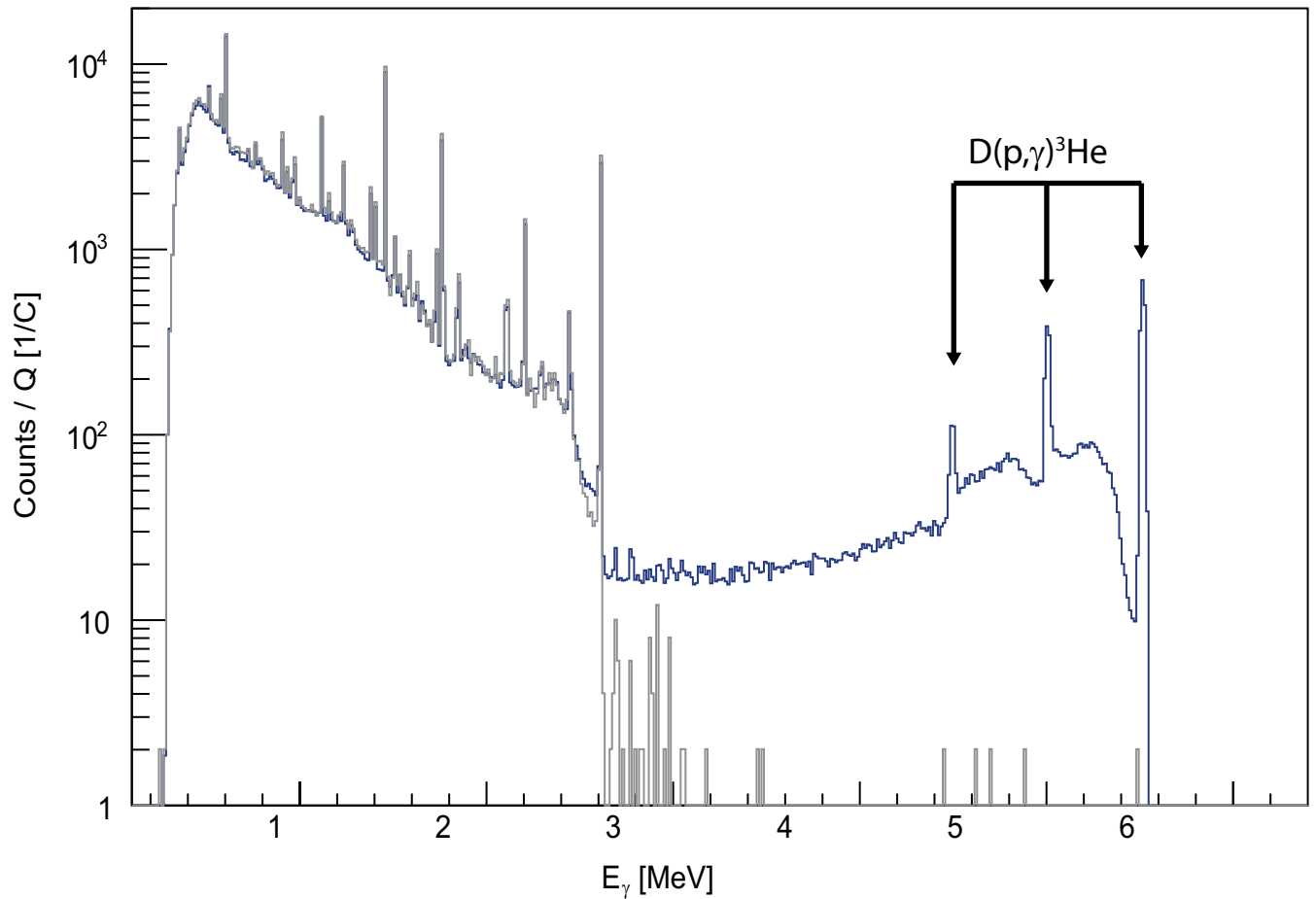
Additional information

Supplementary information is available for this paper at <https://doi.org/10.1038/s41586-020-2878-4>.

Correspondence and requests for materials should be addressed to C.G. or S.Z.

Peer review information Nature thanks Grigory Rogachev and the other, anonymous, reviewer(s) for their contribution to the peer review of this work. Peer reviewer reports are available.

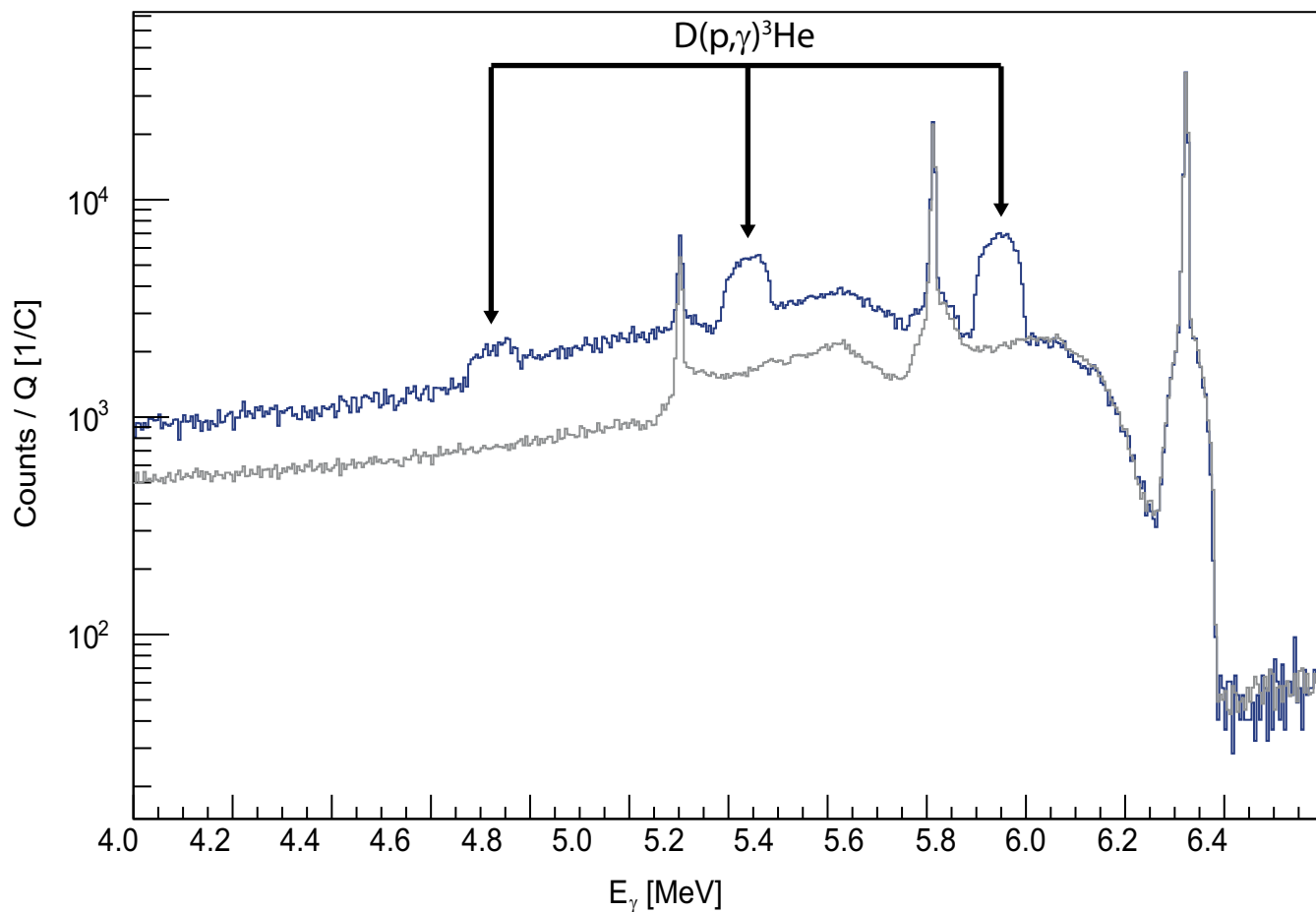
Reprints and permissions information is available at <http://www.nature.com/reprints>.



Extended Data Fig. 1 | Typical γ -ray spectrum obtained underground with the high-purity germanium detector at proton beam energy $E_p = 50$ keV.

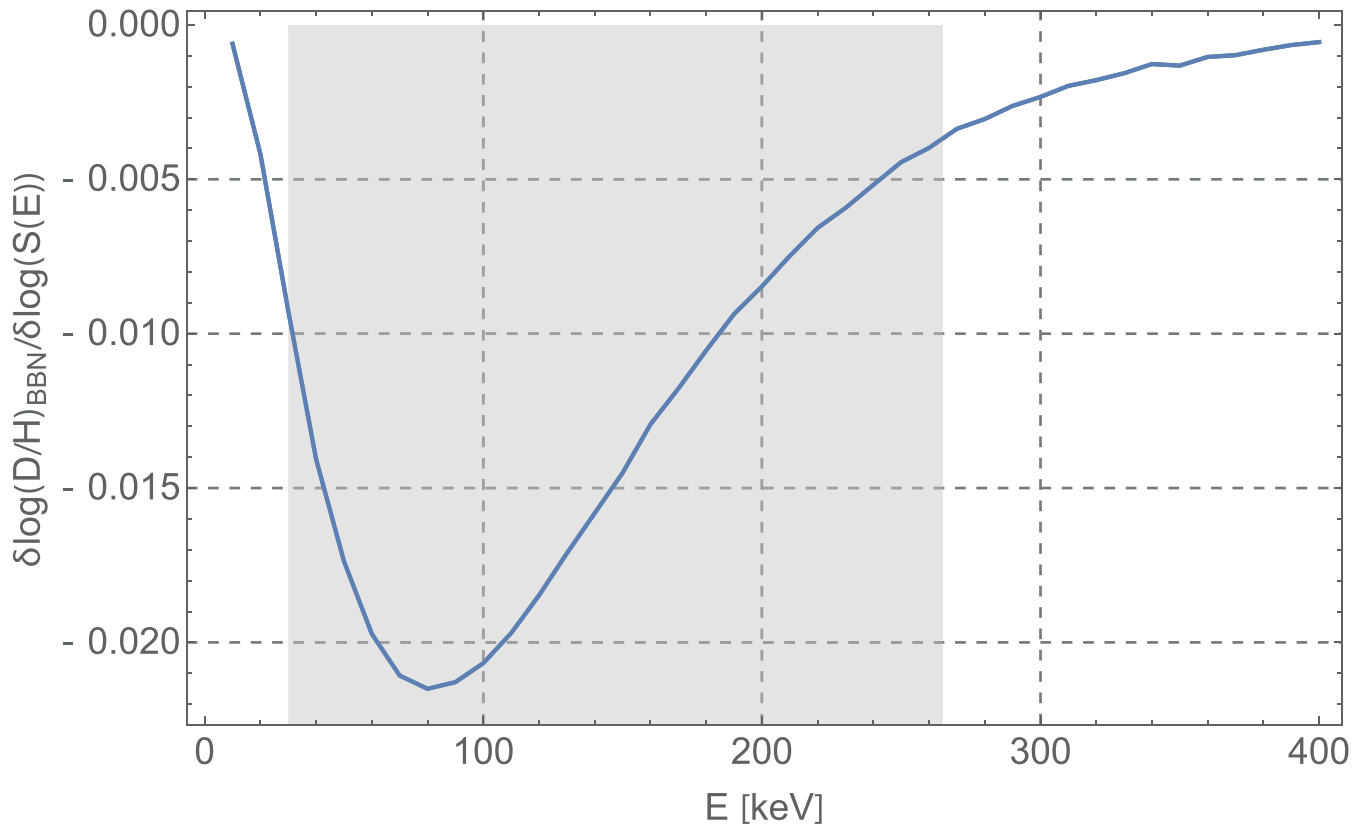
Typical γ -ray spectrum (blue) obtained with the deuterium gas target at $P = 0.3$ mbar, clearly showing the full-energy, single-escape and double-escape peaks from the $D(p,\gamma)^3\text{He}$ reaction. The continuum is mainly due to Compton scattering events in which photons deposit only part of their energy in the

detector. In grey is the beam-induced background spectrum acquired in the control run under the same experimental conditions but with an inert ^4He gas target. Both spectra are normalized to the integrated beam current. The region of interest ($E_\gamma \approx 4.5$ – 5.8 MeV) is essentially background free owing to the million-fold shielding⁸ from cosmic-ray muons attained at the LUNA underground laboratory.



Extended Data Fig. 2 | Typical γ -ray spectrum taken at proton beam energy $E_p = 395$ keV. In blue is the γ -ray spectrum obtained with the deuterium gas target at $P = 0.3$ mbar (the peaks from the $D(p,\gamma)^3\text{He}$ reaction are broadened by the Doppler effect at this higher beam energy). In grey is the beam-induced

background spectrum (acquired with an inert ^4He gas target) due to the ^{19}F contaminant (see text). Its contribution was subtracted leading to net counts on the full-energy peak with a statistical uncertainty of 0.9%. Both spectra are normalized to the integrated beam current.



Extended Data Fig. 3 | Sensitivity of the primordial deuterium abundance to the $D(p,\gamma)^3\text{He}$ reaction cross-section as a function of centre-of-mass energy. The greatest sensitivity is obtained around $E=80$ keV, where

underground measurements are especially effective. The grey area represents the energy region explored at LUNA (see Methods for details).

Extended Data Table 1 | Astrophysical S factors for the $D(p,\gamma)^3\text{He}$ reaction at the measured centre-of-mass energies

E [keV]	S(E) [eV b]	σ_{stat} [eV b]	σ_{syst} [eV b]
32.4	0.386	0.014	0.010
66.7	0.627	0.009	0.016
99.5	0.850	0.008	0.021
115.9	0.966	0.009	0.024
132.9	1.133	0.004	0.031
149.3	1.223	0.006	0.031
166.1	1.375	0.004	0.036
182.7	1.475	0.006	0.037
199.5	1.648	0.003	0.043
222.8	1.791	0.006	0.045
232.9	1.866	0.012	0.051
252.9	2.073	0.012	0.052
262.9	2.156	0.020	0.054

Values of the astrophysical S factor as measured at LUNA over the full energy range explored. Statistical (σ_{stat}) and systematic (σ_{syst}) uncertainties at the 68% confidence level are also reported. The statistical uncertainty is typically negligible except at the lowest energy point (3.6%), where it dominates over the systematic uncertainty (2.7%). Systematic uncertainties remain below 3% at all energies.

Extended Data Table 2 | Thermonuclear reaction rate for the $D(p,\gamma)^3\text{He}$ reaction

T [GK]	R [$\text{cm}^3 \text{mol}^{-1} \text{s}^{-1}$]	R_{low} [$\text{cm}^3 \text{mol}^{-1} \text{s}^{-1}$]	R_{high} [$\text{cm}^3 \text{mol}^{-1} \text{s}^{-1}$]
0.001	1.37×10^{-11}	1.35×10^{-11}	1.39×10^{-11}
0.005	2.57×10^{-5}	2.53×10^{-5}	2.62×10^{-5}
0.01	1.53×10^{-3}	1.51×10^{-3}	1.56×10^{-3}
0.05	9.08×10^{-1}	8.94×10^{-1}	9.22×10^{-1}
0.1	5.74	5.65	5.84
0.5	1.29×10^2	1.26×10^2	1.32×10^2
1.0	3.63×10^2	3.52×10^2	3.74×10^2
1.5	6.32×10^2	6.09×10^2	6.56×10^2
2.0	9.20×10^2	8.79×10^2	9.62×10^2
3.0	1.52×10^3	1.43×10^3	1.61×10^3
4.0	2.11×10^3	1.95×10^3	2.28×10^3
5.0	2.67×10^3	2.40×10^3	2.93×10^3
6.0	3.16×10^3	2.76×10^3	3.55×10^3
7.0	3.56×10^3	3.00×10^3	4.12×10^3
8.0	3.85×10^3	3.09×10^3	4.61×10^3
9.0	4.01×10^3	3.02×10^3	5.01×10^3
10.0	4.02×10^3	2.75×10^3	5.30×10^3

Values of the thermonuclear reaction rate R obtained from our best-fit S factor of the $D(p,\gamma)^3\text{He}$ reaction as a function of temperature in GK. Low and high rates are quoted at the 1σ level.